DarkShake-DVS: Event-based Human Action Recognition under Low-light and Shaking Camera Conditions

Supplementary Material

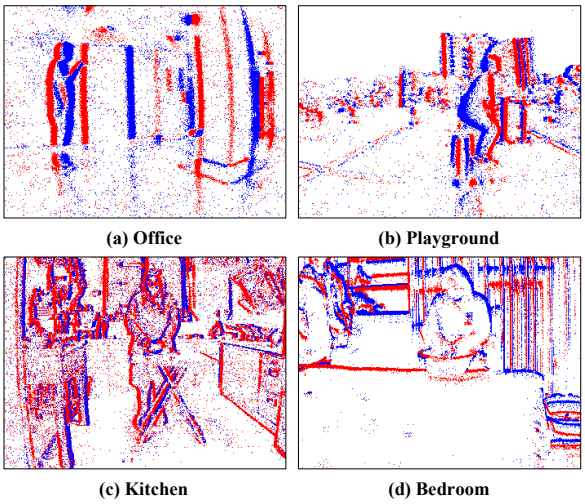

Figure 1. Visualization of representative recording scenes, including offices, playgrounds, kitchens, and bedrooms.

1. More Details of Dataset

Visualization of Categories, Scenes, and Viewpoints. To provide a comprehensive overview of the DarkShake-DVS dataset and substantiate the descriptions in the main paper, we present detailed visualizations of the data distribution. First, the complete list of all action categories is enumerated in Tab. 1. To demonstrate the environmental diversity mentioned in the main text, Fig. 1 displays representative samples from various recording environments, including offices, playgrounds, kitchens, and bedrooms, containing both static and dynamic background elements. Furthermore, to illustrate the extensive geometric coverage, Fig. 2 showcases samples captured from multiple distinct viewpoints. As described in the collection process, these include the front, back, left, right, and four diagonal directions, ensuring the dataset covers a full spectrum of observation angles under realistic 6-DoF camera motion.

Illumination Condition Details. To quantitatively assess the low-light conditions of our DarkShake-DVS dataset, we measured the ambient illumination using a DLX-SL138 digital lux meter. The measurements confirmed an average illuminance of 1-3 Lux across our recording scenes. This illuminance level verifies that the dataset was captured under significant low-light conditions. For traditional frame-based cameras, such low illumination would drastically reduce the signal-to-noise ratio (SNR) and lead to severe motion blur [2, 3, 5, 7], especially when combined with the 6-DoF motion central to our work [1]. However, as discussed in the main paper, event cameras possess high dynamic range [6] and high low-light sensitivity [4] . They operate by capturing microsecond-level relative changes in brightness rather than absolute illumination. Therefore, while an environment of 1-3 Lux is challenging for traditional cameras, it

Algorithm 1 Adaptive IMU Grouping and Scaling Algorithm

Input: IMU angular velocity sequence $\boldsymbol{\omega} = \{\omega_1, \ldots, \omega_T\}$, IMU timestamps $\mathbf{t}$, Thresholds T_{stable}, $N_{\min}$, $N_{\max}$.
textbfOutput: Set of compensation groups $\mathcal{G} = \{G_1, \ldots, G_M\}$, Scaling factors $\boldsymbol{\gamma}$.

Stage 1: Initial Segmentation
Initialize $\mathcal{G}_{\text{raw}} \leftarrow \emptyset$
for each timestamp t **do**
  if $|\omega_t| \leq T_{\text{stable}}$ **then**
    Mark ω_t as *Stable*; group consecutive stable points into $\mathcal{G}_{\text{raw}}$.
  else
    Mark ω_t as *Active*; group consecutive active points into $\mathcal{G}_{\text{raw}}$.
  end if
end for
Stage 2: Hierarchical Refinement (for Active Groups)
Initialize $\mathcal{G}_{\text{refined}} \leftarrow \emptyset$
for each group $G \in \mathcal{G}_{\text{raw}}$ where type is *Active* **do**
  {Step 2.1: Split by Polarity}
  Split G into sub-segments $\{S_1, \ldots\}$ where $\text{sgn}(\omega)$ is constant.
  for each sub-segment $S \in \{S_1, \ldots\}$ **do**
    {Step 2.2: Split by Extrema (Peak)}
    Find peak index $k = \arg\max_{t \in S} |\omega_t|$.
    Split S into $S_{\text{acc}} = S[0:k]$ and $S_{\text{dec}} = S[k+1:end]$.
    for each phase $P \in \{S_{\text{acc}}, S_{\text{dec}}\}$ **do**
      {Step 2.3: Split by Cumulative Energy}
      Calculate total energy $E = \sum |\omega_t|$.
      Find split point j where $\sum_{t=0}^{j} |\omega_t| \approx E/2$.
      Split P into $P_{\text{early}}, P_{\text{late}}$ at index j.
      Add $P_{\text{early}}, P_{\text{late}}$ to $\mathcal{G}_{\text{refined}}$.
    end for
  end for
end for
Add *Stable* groups from $\mathcal{G}_{\text{raw}}$ directly to $\mathcal{G}_{\text{refined}}$.
Stage 3: Temporal Regularization & Scaling
Sort $\mathcal{G}_{\text{refined}}$ by time.
Merge: Combine adjacent groups if length $< N_{\min}$.
Split: Recursively divide groups if length $> N_{\max}$.
Calculate: For each final group G_k, compute γ_k:
$\gamma_k \leftarrow \gamma_{\min} + \frac{\gamma_{\max} - \gamma_{\min}}{a \cdot |G_k| + b}$
return Final Groups $\mathcal{G}$, Scaling Factors $\boldsymbol{\gamma}$

No.	Class	No.	Class	No.	Class	No.	Class	No.	Class
1	Holding head	2	Holding stomach	3	Waving	4	Standing up	5	Pulling door
6	Drinking	7	Walking stooped	8	Walking holding wall	9	Sitting down	10	Squatting
11	Crossing arms	12	Sitting down	13	Bowing holding wall	14	Punching	15	Running
16	Holding back of head	17	Walking down stairs	18	Reading book	19	Picking up chair	20	Waving both hands
21	Sweeping	22	Dancing	23	Cutting vegetables	24	Stir-frying	25	Brushing hair
26	Wiping face	27	Knitting sweater	28	Washing face	29	Washing clothes	30	Beating quilt
31	Clapping	32	Putting hands on hips	33	Shaking hands	34	Saluting	35	Sitting down (paired)
36	Fist bumping	37	Hitting	38	Performing CPR	39	Giving chair and sitting down	40	Playing tug of war
41	Reading (paired)	42	High fiving	43	Hugging	44	Rock-paper-scissors	45	Holding umbrella
46	Typing	47	Playing football	48	Walking arm on shoulder	49	Putting on hat	50	Kicking
51	Following	52	Patting shoulder	53	Arm wrestling	54	Cutting hair	55	Playing handball
56	Swinging jump rope	57	Dancing in pairs	58	Hammering nail	59	Repairing bicycle	60	Doing burpees (paired)
61	Latin dancing	62	Shaking out clothes						

Table 1. Full list of the 62 action categories in the DarkShake-DVS dataset.

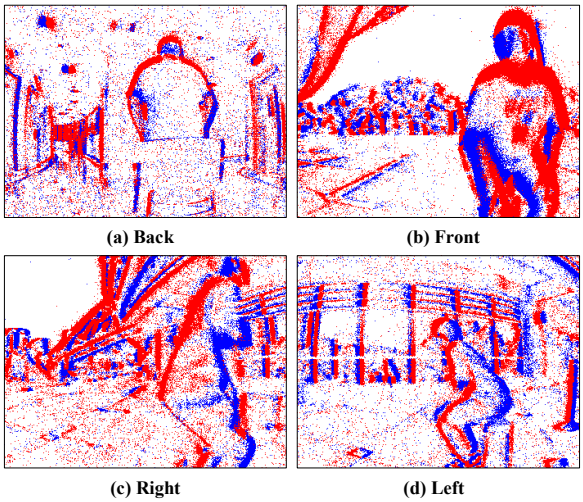

(a) Back **(b) Front** **(c) Right** **(d) Left**

Figure 2. Visualization of samples from diverse viewpoints, including front, back, side, and diagonal angles.

represents an ideal regime that is effectively captured by event cameras, highlighting their advantages in low-noise signal acquisition. This makes our dataset a robust and realistic benchmark for evaluating the performance of HAR methods in challenging real-world low-light scenarios.

Event–IMU Complementarity In our work, pairing the event camera with an IMU is crucial for addressing the challenge of 6-DoF motion. Unconstrained camera shake generates a high volume of background events, which contaminate the foreground events caused by the human action, severely interfering with recognition. The unique advantage of the IMU is its ability to independently and accurately measure the camera's own motion , such as angular velocity and acceleration, with performance that is completely unaffected by lighting conditions. In our low-light dataset, where visual-only motion estimation algorithms would fail, the IMU consistently provides reliable motion data. Therefore, we can leverage the precise ego-motion information from the IMU to compensate and stabilize the event stream, thereby isolating the true human action. This tight coupling of Event-IMU data is an industry and academic consensus; many advanced commercial event cameras, such as the DVXplorer natively integrate an IMU, confirming the validity of our method and dataset design.

Data Collection and Ethics. Taking into account the sensitive nature of our dataset, all data involving human participants were collected in accordance with informed consent procedures. Participants were fully informed about the purpose of the study, the nature of their participation, potential risks, benefits, and their right to withdraw from the study at any time without suffering any adverse consequences.

2. Parameter Settings

Adaptive Motion Compensation. In the proposed IMU-temporal-aware dynamic scaling mechanism, the scaling factor γ_{group} is adjusted based on the IMU sample density N_{imu}. The bounds for the scaling factor are set to $\gamma_{\min} = 2$ and $\gamma_{\max} = 5$. The tuning coefficients in the denominator, which control the sensitivity of the scaling to the sample count, are set to $a = 0.15$ and $b = 3$, respectively. These values were empirically determined to balance motion suppression and feature preservation.IGS Algorithm. In the Informative Group Sampling (IGS) strategy, the comprehensive score $S_{\text{comb}}(i)$ is a weighted sum of four metrics: relevance, quality, uniformity, and diversity. We assign the weights as follows: the relevance weight $w_{\text{rel}} = 0.1$, the quality weight $w_{\text{q}} = 0.1$, the uniformity weight $w_{\text{u}} = 0.6$, and the diversity weight $w_{\text{d}} = 0.1$. The higher weights on uniformity are higher, indicating that we prioritize semantic alignment during the frame selection process.

Detailed Algorithm for Adaptive Motion Compensation. To provide a comprehensive understanding of our adaptive motion compensation framework, we present the detailed algorithmic procedure for IMU data grouping and dynamic scaling factor calculation. As described in the main paper, our goal is to partition the continuous angular velocity sequence into fine-grained, motion-consistent groups. While the main text outlines the frequency-domain conceptualization, the practical implementation involves a hierarchical segmentation strategy followed by a regularization process.The specific grouping process, as outlined in Algorithm 1, consists of three primary stages. (1) Initial Seg-

mentation: We first separate the IMU sequence into "stable" and "active" segments based on a noise threshold (set to ± 3 rad/s in our experiments). Stable regions represent static or micro-motion phases, while active regions contain significant camera ego-motion. (2) Hierarchical Refinement: For active segments, we apply a three-step refinement to capture motion dynamics: Sign-based Splitting ensures each group maintains a monotonic direction; Extrema-based Splitting divides the motion into acceleration and deceleration phases by cutting at the peak angular velocity; and Energy-based Splitting further subdivides high-energy segments at the median point of their cumulative angular displacement (energy), ensuring a balanced motion distribution within groups. (3) Temporal Regularization: To satisfy the temporal constraints of the event camera, we perform a post-processing step where groups smaller than a minimum duration (N_{min}) are merged into adjacent groups, and groups exceeding a maximum duration (N_{max}) are recursively split. Finally, the dynamic scaling factor γ_{group} is computed for each valid group to guide the event warping process.

References

[1] Sandy ST Hutagalung, Kevin C Simalango, Samuel Lumbantobing, et al. The effectiveness of opencv based face detection in low-light environments. *Journal of Informatics and Telecommunication Engineering*, 7(1):209–220, 2023. 1

[2] Kunchang Li, Xinhao Li, Yi Wang, Yinan He, Yali Wang, Limin Wang, and Yu Qiao. Videomamba: State space model for efficient video understanding. In *European conference on computer vision*, pages 237–255. Springer, 2024. 1

[3] Ze Liu, Jia Ning, Yue Cao, Yixuan Wei, Zheng Zhang, Stephen Lin, and Han Hu. Video swin transformer. In *Proceedings of the IEEE/CVF conference on computer vision and pattern recognition*, pages 3202–3211, 2022. 1

[4] Liyuan Pan, Cedric Scheerlinck, Xin Yu, Richard Hartley, Miaomiao Liu, and Yuchao Dai. Bringing a blurry frame alive at high frame-rate with an event camera. In *Proceedings of the IEEE/CVF Conference on Computer Vision and Pattern Recognition (CVPR)*, 2019. 1

[5] Xiao Wang, Zongzhen Wu, Bo Jiang, Zhimin Bao, Lin Zhu, Guoqi Li, Yaowei Wang, and Yonghong Tian. Hardvs: Revisiting human activity recognition with dynamic vision sensors. In *Proceedings of the AAAI Conference on Artificial Intelligence*, pages 5615–5623, 2024. 1

[6] Yan Yang, Liyuan Pan, and Liu Liu. Event camera data dense pre-training. In *Computer Vision – ECCV 2024*, pages 292–310, Cham, 2025. Springer Nature Switzerland. 1

[7] Zhaokun Zhou, Yuesheng Zhu, Chao He, Yaowei Wang, Shuicheng YAN, Yonghong Tian, and Li Yuan. Spikformer: When spiking neural network meets transformer. In *The Eleventh International Conference on Learning Representations*. 1